Photoinduced electron transfer from zinc tetraphenylporphyrin to 2-nitrofluorene in polar solvent acetonitrile

ARTICLE *in* JOURNAL OF PHOTOCHEMISTRY AND PHOTOBIOLOGY A CHEMISTRY · JUNE 2015

Impact Factor: 2.5 · DOI: 10.1016/j.jphotochem.2015.03.019

Journal of Photochemistry and Photobiology A: Chemistry 306 (2015) 55–65

Contents lists available at ScienceDirect

Journal of Photochemistry and Photobiology A: Chemistry

journal homepage: www.elsevier.com/locate/jphotochem

Photoinduced electron transfer from zinc tetraphenylporphyrin to 2-nitrofluorene in polar solvent acetonitrile

Mihir Ghosh [a], Aruna K. Mora [b], Sukhendu Nath [b], P. Hemant Kumar [c], Prakriti Ranjan Bangal [c], Subrata Sinha [a,*]

[a] Integrated Science Education and Research Centre, Siksha-Bhavana, Visva-Bharati, Santiniketan 731 235, India
[b] Radiation & Photochemistry Division, Bhabha Atomic Research Centre, Trombay, Mumbai 400 085, India
[c] Inorganic and Physical Chemistry Division, Indian Institute of Chemical Technology, Hyderabad 500 607, India

ARTICLE INFO

Article history:
Received 15 January 2015
Received in revised form 20 March 2015
Accepted 23 March 2015
Available online 25 March 2015

Keywords:
Zinc tetraphenylporphyrin
2-Nitrofluorene
Electron transfer
Marcus theory

ABSTRACT

The possibility of intermolecular photoinduced ET (PET) is investigated in a novel donor–acceptor (D–A) system consisting of zinc tetraphenylporphyrin (ZnTPP) as donor and 2-nitrofluorene (2NF) as acceptor upon photoexcitation of the former moieties in polar solvent acetonitrile (ACN). The observed values (7.23×10^9 L/(mol s) and 7.04×10^9 L/(mol s)) of the fluorescence quenching rate constant from steady state and time-resolved data, respectively, are in good agreement with that (5.65×10^9 L/(mol s)) obtained from Marcus theory. Excited state absorption (ESA) from the S_2 state of Soret excited ZnTPP to higher electronic states gives rise to broad transient absorption spectra in 560–700 nm region. Presence of 2NF leads to a faster decay (up to 100 ps time delay) of the ESA signal of ZnTPP at a probe wavelength of 620 nm. This indicates ultrafast ET from the S_2 state (zero vibrational level) as well as the higher vibrational levels of the S_1 state of ZnTPP to 2NF. Moreover, transient absorption kinetics at longer time delays (up to 7 ns) at a probe wavelength of 620 nm show the formation of a charge separated state due to ET from the S_1 state (zero vibrational level) of the Soret excited ZnTPP to 2NF.

1. Introduction

Porphyrins play very important roles in biological electron transfer (ET) processes such as photosynthesis and respiration [1–7]. Chlorophylls, which are porphyrin derivatives, play a crucial role in natural photosynthesis for converting solar energy into chemical energy [1,8,9]. In order to develop artificial photosynthetic systems and organic photovoltaic cells, photoinduced ET (PET) and energy transfer processes have been studied extensively in porphyrin based donor–acceptor (D–A) systems [10–26]. The unique structural, photochemical and electrochemical properties of porphyrins make them useful for a variety of potential applications such as dye sensitized solar cells (DSSCs) [27–29], non-linear optics [30], telecommunication technologies [31], gas sensors [32], photochromic recording medium [33], catalysts in industrial processes [34,35], anticancer pharmaceutical drugs [36], photodynamic destruction of viruses [37,38], photodynamic therapy (PDT) [39,40], etc.

Porphyrins are cyclic molecules composed of four smaller 5-membered heterocycles, called pyrroles, each one containing one nitrogen and four carbon atoms. The electronic absorption spectra of a free base porphyrin consist of an intense band at about 400 nm, called Soret band (or B band) and four weaker bands in the visible region (about 500–700 nm), called Q bands. The Soret and Q bands are due to π–π^* transitions from the ground singlet state to the second excited singlet state ($S_0 \rightarrow S_2$) and from the ground singlet state to the first excited singlet state ($S_0 \rightarrow S_1$), respectively. Metalation of free base porphyrin increases the ring microsymmetry from D_{2h} to D_{4h} accompanied by a decrease of the number of Q bands from four to two [1,41]. The internal conversion from S_2 to S_1 is rapid and hence fluorescence is usually observed from the S_1 state with a quantum yield $\sim 10^{-2}$ [42–44]. However, very weak fluorescence is observed from the S_2 state of porphyrins with a quantum yield $\sim 10^{-4}$ [19,20].

Among the various porphyrin derivatives, zinc tetraphenylporphyrin (ZnTPP) is one of the most extensively studied molecule so far mainly due to its good solubility in many commonly used organic solvents. Extensive studies on inter- and intramolecular PET have been carried out by many research groups in ZnTPP based D–A systems with various acceptors. Kuciauskas et al. [11] observed the transient absorption spectra of zinc porphyrin radical

* Corresponding author. Tel.: +91 3463 261029; fax: +91 3463 261029.
E-mail address: subratasinha67@rediffmail.com (S. Sinha).

http://dx.doi.org/10.1016/j.jphotochem.2015.03.019
1010-6030/

cation showing the formation with a time constant of 1.9 ps and decay with a lifetime of 50 ps in a covalently linked ZnTPP – fullerene (C_{60}) dyad. They concluded that the charge separated (CS) state lives for 50 ps in the dyad. Bell et al. [12] observed long-range PET in a dyad containing ZnTPP donor and C_{60} acceptor separated by a saturated norbornylogous bridge nine sigma bonds in benzonitrile (BN). They found that the CS state exhibits a long lifetime of 420 ns. Bahr et al. [13] investigated PET in a carotene(C)–ZnTPP–C_{60} molecular triad in 2-methyltetrahydrofuran (MTHF). They observed that excitation of ZnTPP leads to primary ET from ZnTPP to C_{60} and then secondary ET from carotene to $ZnTPP^+$, thereby forming a final CS state of C^+–ZnTPP–C_{60} – with a lifetime of 69 ns. Luo et al. [14] reported sequential PET in a ZnTPP–TPP–C_{60} triad in BN to form a final CS state of $ZnTPP^+$–TPP–C_{60} – with a lifetime of 21 μs. Also, they observed formation of a long-lived (580 ns) CS state in a ZnTPP–C_{60} reference dyad. Imahori et al. [15,16] studied photoinduced charge separation and recombination processes in various TPP and ZnTPP based dyads and triads. They observed broad transient absorption spectra of ZnTPP radical cation and a long-lived (16 μs) CS state in ferrocene–ZnTPP–C_{60} triad [15]. Bell et al. [17] reported CS state in a giant ZnTPP-bridge-C_{60} system with a lifetime of 460 ns accompanied by the observation of a broad transient absorption spectra of ZnTPP radical cation in the 600–700 nm region. Boom et al. [18] prepared a large molecule in which four perylene-3.4:9,10-tetracarboxydiimide (PDI) molecules are attached to a central ZnTPP molecule. Photoexcitation of ZnTPP–PDI at the Soret band of ZnTPP results in the formation of a CS state with a time constant of 15 ps and decay lifetime of 5.3 ns. Yu et al. [19] reported ultrafast (<100 fs) ET from Soret band excited ZnTPP to dichloromethane solvent for a subset of excited ZnTPP molecules in favorably oriented contact with the solvent molecules. Hayes et al. [21] reported competitive ET from the S_2 and S_1 excited states of ZnTPP to a covalently bound pyromellitimide in MTHF and toluene solvents. Also, they observed broad transient absorption spectra of ZnTPP radical cation in 600-700 nm region. Zeyada et al. [23] investigated the transport mechanisms and photovoltaic properties of ZnTPP/n-type silicon heterojunction solar cells. Kanematsu et al. [24] studied the dynamics of intermolecular ET reactions of planar and nonplanar Al^{III} porphyrins with an axial ligand ($PhCOO^-$) using a series of *p*-benzoquinone derivatives as electron acceptors in comparison with the corresponding Zn^{II} porphyrins (including ZnTPP). Robotham et al. [25] investigated PET in a covalently linked ZnTPP–amino naphthaline diimide (ANDI) dyad in BN and toluene solvents. They reported that upon Soret band excitation of ZnTPP, fast ET occurs from the S_2 state to ANDI followed by rapid charge recombination to form S_1 state of ZnTPP that subsequently undergoes a further slower ET to ANDI.

The aim of the present work is to investigate the possibilities and consequences of intermolecular PET in a novel D–A system consisting of ZnTPP as donor and 2-nitrofluorene (2NF) as acceptor in polar solvent acetonitrile (ACN, static dielectric constant $\varepsilon_s = 37.5$) by using steady state and time-resolved spectroscopic measurements. 2NF is a well known electron acceptor [45–48]. It is a small organic molecule and quite cheaply available in the market. However, earlier ET studies of 2NF as an acceptor with various donors (dimethyl susbstituted phenols, tatrahydronaphthols, methylindoles etc.) showed concurrent occurrences of electron and energy transfer processes [45–48]. Such D–A systems are not suitable from application point of view as proper analysis of the fluorescence quenching data in terms of electron and energy transfer processes is often very difficult. In the present investigations, fluorescence (intensity as well as lifetime) quenching of ZnTPP is observed in presence of the quencher 2NF indicating the possibility of PET in this D–A system in polar solvent ACN by avoiding the competitive singlet–singlet energy transfer process. The occurrence of PET in the presently used D–A system is further confirmed by the data obtained from femtosecond transient absorption measurements based on pump-probe technique.

2. Experimental

2.1. Chemicals

The samples ZnTPP (5,10,15,20-tetraphenyl-21H,23H-porphine zinc) and 2NF (Fig. 1) were used as supplied by Sigma–Aldrich. The solvent ACN of spectroscopic grade was purchased from Sigma–Aldrich and was tested before use to check any impurity emission in the wavelength region studied.

2.2. Instruments

The steady state electronic absorption spectra of the samples were recorded at the ambient temperature (300 K) by using 1 cm path length rectangular quartz cuvette by means of JASCO V-650 absorption spectrophotometer. Steady state fluorescence spectra of the samples were recorded by using JASCO FP-6500 fluorescence spectrometer at 300 K. Emission was detected at right angles to the direction of excitation light in order to avoid stray light.

The time-resolved fluorescence measurements were carried out by using a time correlated single photon counting (TCSPC) spectrometer from IBH (UK). The sample was excited with 560 nm light from a diode laser with 1 MHz repetition rate. A PMT based detector (TBX4, IBH) was used for detection of the emitted photons through a monochromator. The instrument response of the TCSPC set-up was measured by collecting the scattered light from a TiO_2 suspension in water. The instrument response function thus measured was ~200 ps. The decays were analyzed using IBH DAS-6 analysis software. The reduced χ^2, Durbin–Watson (DW) parameter and residuals were used to judge the goodness of the fit.

For the pump-probe transient absorption measurements, a mode-locked automated broadband (tuning from 690 nm to 1040 nm) Ti:sapphire laser (Mai Tai HP, Spectra Physics), pumped by 14 W frequency doubled ND:YVO_4 (532 nm), was used as master oscillator. It produces laser pulses of <100 fs duration (full width at half-maximum, FWHM) and ~31 nJ (energy/pulse) centered at

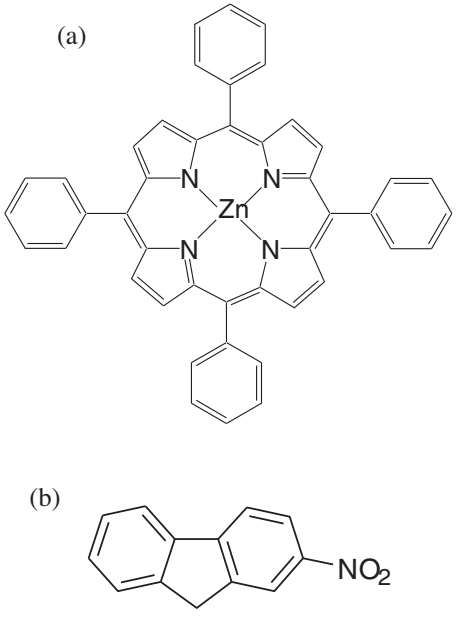

Fig. 1. Molecular structures of (a) ZnTPP and (b) 2NF.

800 nm (80 MHz repetition rate) with average power 2.5 W. A part of this fundamental pulsed laser beam were stretched in a grating stretcher and amplified at 1 kHz using a Ti:sapphire regenerative amplifier (Spitfire Ace Spectra Physics) pumped by the second harmonic (527 nm, 30 W) from intercavity-doubled, diode-pumped Q-switched ND:YLF laser (Empower-30 Spectra Physics). Compression of the amplified pulses yielded >4 mJ pulses centered at 800 nm having an FWHM of <120 fs. Part of this amplified fundamental beam was seed into OPA (TOPAS Prime) to create pump source of required wavelength for pump-probe experiment and another part of this fundamental beam (100 mW) was steered to generate a white-light continuum for generating probe pulse for transient absorption experiment. To perform pump-probe experiment, transient spectrometer of CDP Corporation (Excipro) was used. The output of TOPAS prime was used as pump source at required wavelength and fed into spectrometer through synchronized chopper for 1 kHz repetition rate. A lens (f = 200 mm) was used to adjust the pump diameter while an iris and neutral density filter combination were used to adjust the pump energy. A Berek's variable wave plate was placed in the pump beam for polarization and continuum chirp measurement. A part of the (1 kHz repetition rate) amplified fundamental beam (100 mW, 800 nm) was fed to the spectrometer focused onto a thin rotating (2 mm) CaF_2 crystal window to generate a white-light continuum and a fraction of this beam was sent to a photodetector, which controls speed and phase of the chopper rotation. The beam of white light was collimated with parabolic mirror (f = 50 mm, 90°). Suitable aperture cut the central part of the white light continuum and a suitable filter eliminated the fundamental light. Then this white light was reflected from a beam splitter and mirror into two identical probe and reference beams. Two concave mirrors (f = 150 nm) were used to focus both probe and reference beams to the rotating sample cell. Two lenses (f = 60 mm) made probe and reference images at the entrance surfaces of two optical fibers, which are connected to the entrance slit of the imaging spectrometer (CDP2022i). This spectrometer consists of UV–visible photodiode (Si linear photodiode) arrays and IR Photodiode (GaAs linear photodiode) array with spectral response range 200–1000 nm and 900–1700 nm, respectively.

3. Results and discussion

3.1. Steady state absorption measurements

Fig. 2 shows the steady state absorption spectra of ZnTPP and 2NF in ACN at the ambient temperature (300 K). The absorption spectra of ZnTPP consist of an intense S_2 band (peak at 421 nm) and a weak S_1 band (peaks at 556 nm and 595 nm). The absorption spectra of 2NF show a peak at 332 nm due to $S_0 \rightarrow S_1$ transition. These are well-known features of the present donor and acceptor molecules [22,45]. It is to be mentioned that the ZnTPP–2NF system is found not to form any ground state complexation in ACN even at higher concentrations of the quencher 2NF as used in the fluorescence quenching measurements (vide infra).

3.2. Gibbs free energy change

The possibility of the occurrence of PET between an electron donor and an acceptor can be calculated by using the Rehm–Weller relation (Eq. (1)) [49].

$$\Delta G^0 = e\left[E^{OX}_{1/2}\left(\frac{D}{D^+}\right) - E^{RED}_{1/2}\left(\frac{A^-}{A}\right)\right] - E^*_{0,0} - \frac{e^2}{(4\pi\varepsilon_0\varepsilon_s R)} \quad (1)$$

here ΔG^0 is the Gibbs free energy change associated with the ET reaction. $E^{OX}_{1/2}(D/D^+)$ and $E^{RED}_{1/2}(A^-/A)$ are half-wave oxidation potential of the donor and half-wave reduction potential of the acceptor, respectively. $E^*_{0,0}$ is the (0,0) energy (2.084 eV corresponding to 595 nm, Fig. 2) of the fluorophore ZnTPP. The last term on the right hand side of Eq. (1) is the Coulomb term, where R is the distance between oxidized donor and reduced acceptor. The value of R is usually taken as the sum of the radii of oxidized donor and reduced acceptor. The radii of the donor ZnTPP and acceptor 2NF are taken as 8.8 Å and 5.1 Å, respectively. The radii are computed by using MOPAC-CI (6 × 6) version 5 package with AMI Hamiltonian for the donor and acceptor molecules in their ground states. Further, in Eq. (1), 'e' is the charge of an electron, ε_0 is the vacuum permittivity and ε_s is the dielectric constant of the solvent in which ET reaction takes place. In polar solvent ACN, the Coulomb term is found to be equal to 0.03 eV only. The oxidation potential of ZnTPP is taken as 0.66 V [24,50], while the reduction potential of 2NF is taken as −1.18 V [45]. Therefore, the value of ΔG^0 is found to be equal to −0.274 eV for the present D–A system in ACN (Eq. (1)). The negative value of ΔG^0 ($\Delta G^0 < 0$) indicates that PET from the first excited singlet state of ZnTPP molecules to the ground state of 2NF molecules in ACN is moderately exergonic and hence energetically feasible.

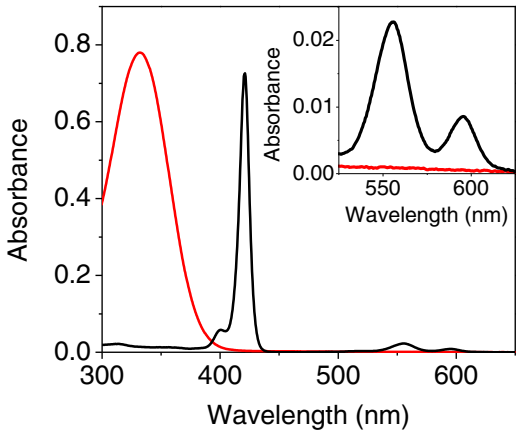

Fig. 2. Steady state absorption spectra of ZnTPP (concentration = 1.4×10^{-6} mol/L, black curve) and 2NF (concentration = 4.4×10^{-5} mol/L, red curve) in ACN at 300 K (path length = 1 cm). The inset shows the Q bands of ZnTPP more clearly. (For interpretation of the references to color in this figure legend, the reader is referred to the web version of this article.)

3.3. Steady state emission measurements

Fig. 3a shows significant quenching of steady state fluorescence emission (peaks at 603 nm and 675 nm) of ZnTPP donor in presence of the acceptor 2NF in ACN at 300 K. In order to selectively excite the donor moity only, ZnTPP is excited at the Q band (556 nm), where 2NF has negligible absorbance (Fig. 2). All the fluorescence measurements are carried out by using dilute solutions (~10^{-5} mol/L) of ZnTPP in order to minimize the self-quenching effect, which is known to deform the emission spectral characteristics of the fluorophore at high concentration [43]. It is to be mentioned that 2NF does not exhibit any fluorescence emission in liquid medium at 300 K upon photoexcitation at 332 nm [45]. Also, overlapping between the donor emission spectra and acceptor absorption spectra is very weak. Hence, the possibility of absorption of the emitted photons from the singlet excited ZnTPP molecules by ground state 2NF molecules (radiative energy transfer or secondary inner filter effect [51]) is very low. However, quite high concentration (~10^{-2}–10^{-3} mol/L) of 2NF is required for appreciable quenching of the steady state emission of ZnTPP. Consequently, inner filter effect (primary as well as secondary) by 2NF on the fluorescence of ZnTPP cannot be avoided completely,

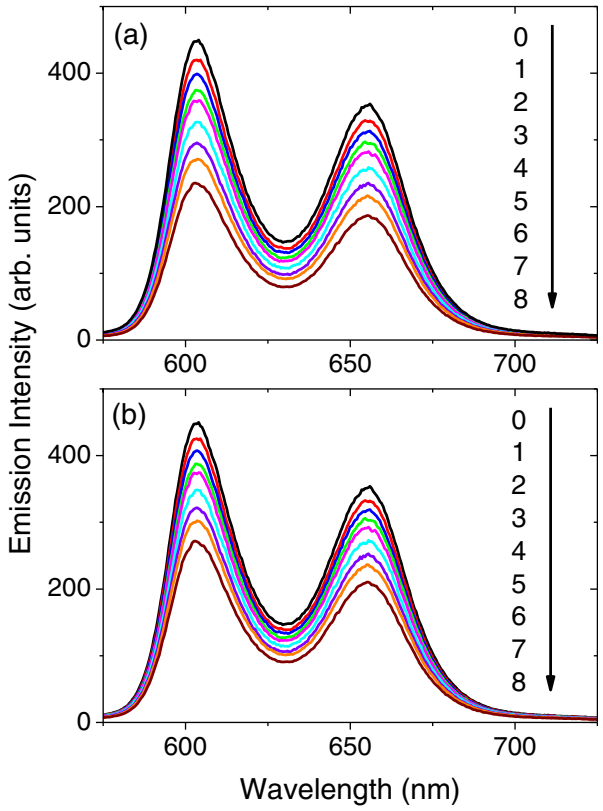

Fig. 3. (a) Uncorrected and (b) corrected (from inner filter effect) steady state fluorescence emission spectra of a mixture of ZnTPP (concentration = 1.78×10^{-5} mol/L) and 2NF in ACN at 300 K (excitation wavelength = 556 nm). Concentration of 2NF (mol/L): (0) 0; (1) 4.27×10^{-3}; (2) 7.12×10^{-3}; (3) 1.14×10^{-2}; (4) 1.43×10^{-2}; (5) 2.13×10^{-2}; (6) 2.85×10^{-2}; (7) 3.60×10^{-2}; (8) 4.80×10^{-2}.

especially on the blue side of the emission spectra. Therefore, the emission spectra of ZnTPP in presence of 2NF are corrected from inner filter effect by using the following relation [51].

$$f_{\text{corrected}} = f_{\text{observed}} \text{antilog}\left(\frac{\text{OD}_{\text{ex}} + \text{OD}_{\text{em}}}{2}\right) \quad (2)$$

here OD_{ex} and OD_{em} are the optical densities (or absorbances) of 2NF at the excitation and emission wavelengths, respectively. As expected, the corrected fluorescence intensities of ZnTPP in presence of 2NF are found to be only slightly higher than the corresponding observed (uncorrected) fluorescence intensities (Fig. 3).

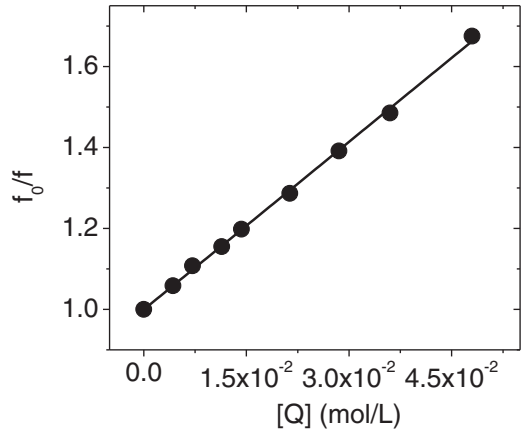

Fig. 4. Stern–Volmer plot from corrected steady state fluorescence emission of ZnTPP in presence of 2NF in ACN at 300 K (excitation wavelength = 556 nm) obtained from Fig. 3b (considering emission intensity of ZnTPP at 603 nm).

Table 1
Fluorescence lifetimes of ZnTPP (concentration = 1.84×10^{-5} mol/L) in absence and in presence of 2NF in ACN at 300 K (excitation wavelength = 560 nm, emission wavelength = 603 nm).

Concentration of 2NF (mol/L)	τ[a] (ns)	χ^2	DW
0	1.91	1.18	1.87
1.01×10^{-2}	1.68	1.21	1.92
2.2×10^{-2}	1.47	0.98	1.93
3.84×10^{-2}	1.26	0.98	1.92

[a] Obtained by single-exponential fitting of the decay curves.

The steady state fluorescence quenching data for the ZnTPP–2NF system in ACN (obtained from the corrected fluorescence spectra in Fig. 3b) are found to follow the linear Stern–Volmer (SV) relation (Eq. (3)) [51] as shown in Fig. 4.

$$\frac{f_0}{f} = 1 + K_{\text{SV}}[Q] \quad (3)$$

here f_0 and f are the relative fluorescence emission intensities of ZnTPP without and with the quencher (2NF) concentration [Q], respectively. K_{SV} ($= k_q \tau_0$) is the SV constant, where τ_0 is the fluorescence lifetime of ZnTPP in absence of 2NF and k_q is the second-order bimolecular fluorescence quenching rate constant. The slope of the linear plot in Fig. 4 gives a value of K_{SV} as 13.81 L/mol. As $\tau_0 = 1.91$ ns (Table 1, vide infra), the observed value of k_q is found to be equal to 7.23×10^9 L/(mol s). Clearly, the observed value of k_q from steady state fluorescence quenching data is slightly less than the second-order diffusion-controlled rate constant of 1.9×10^{10} L/(mol s) in ACN (vide infra). This indicates the possibility of PET in the present D–A system. As already mentioned, there is practically no overlapping between the fluorescence emission spectra of ZnTPP and absorption spectra

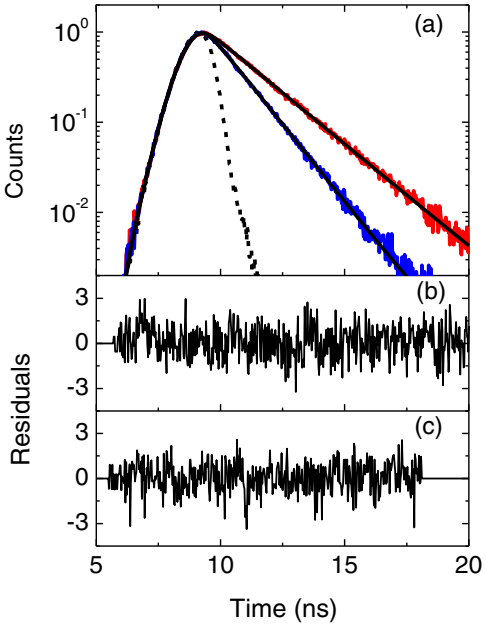

Fig. 5. (a) Normalised fluorescence decay curves of ZnTPP (concentration = 1.84×10^{-5} mol/L) in presence of 2NF in ACN at 300 K (excitation wavelength = 560 nm, emission wavelength = 603 nm). Concentration of 2NF (mol/L): 0 (red curve); 3.84×10^{-2} (blue curve). Solid black lines represent fitted decay curves and dashed black line represents instrument response profile. (b) Residuals for fitting the red decay curve. (c) Residuals for fitting the blue decay curve. (For interpretation of the references to color in this figure legend, the reader is referred to the web version of this article.)

of 2NF in ACN. This excludes the possibility of singlet–singlet energy transfer from the singlet excited ZnTPP molecules to the ground state 2NF molecules.

3.4. TCSPC measurements

Fig. 5 shows the fluorescence decay curves of ZnTPP without and with 2NF (3.84×10^{-2} mol/L) in ACN. ZnTPP is excited at 560 nm (Q band) and the fluorescence decays are monitored at an emission wavelength of 603 nm. Table 1 shows the fluorescence lifetimes of ZnTPP without and with 2NF in ACN obtained by single-exponential fit of the decay curves. It is noteworthy that exactly identical fluorescence lifetimes (compared to those obtained at an emission wavelength of 603 nm, Table 1) of ZnTPP without and with 2NF are obtained by monitoring the fluorescence decays at an emission wavelength of 675 nm. The observed fluorescence lifetime of ZnTPP without 2NF in ACN is 1.91 ns, which tallies quite well with the fluorescence lifetime of the S_1 state of ZnTPP in liquid medium reported in earlier works [44]. Table 1 as well as Fig. 5 show significant quenching of the fluorescence lifetime of ZnTPP with gradual addition of 2NF in ACN. The fluorescence quenching data (Table 1) obtained from TCSPC measurements are fitted with linear SV relation (Eq. (4)) [51] quite satisfactorily as shown in Fig. 6.

$$\frac{\tau_0}{\tau} = 1 + K_{SV}[Q] \tag{4}$$

here τ_0 and τ are the fluorescence lifetimes of ZnTPP in absence and in presence of the quencher 2NF, respectively. The slope of the linear plot in Fig. 6 gives a value of K_{SV} as 13.44 L/mol. As the value of τ_0 for ZnTPP is known (Table 1), the observed value of k_q is found to be equal to 7.04×10^9 L/(mol s), which is slightly less than the diffusion-controlled limit of 1.9×10^{10} L/(mol s) in ACN (vide infra). Again, the value of k_q obtained from TCSPC measurements is nearly the same as that obtained from the steady state measurements. Thus, both steady state and TCSPC measurements indicate the possibility of PET in ZnTPP–2NF system in ACN.

3.5. Marcus theory

The first-order ET rate constant (k_{ET}) can be computed from the Arrhenius relation (Eq. (5)) [52].

$$k_{ET} = A\exp\left(-\frac{\Delta G^*}{k_B T}\right) \tag{5}$$

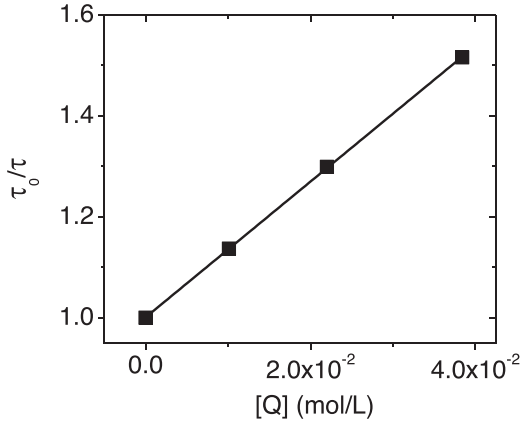

Fig. 6. Stern–Volmer plot from fluorescence lifetime values of ZnTPP in presence of 2NF in ACN at 300 K (excitation wavelength = 560 nm, emission wavelength = 603 nm) obtained from Table 1 (see the text).

Following Rehm and Weller, we treat '*A*' as an effective solution-phase collision frequency so that $A = 1 \times 10^{11}$ s^{-1} [52]. According to Marcus outer-sphere ET theory, activation energy ΔG^* is given by Eq. (6) [52–54].

$$\Delta G^* = \frac{(\Delta G^0 + \lambda)^2}{4\lambda} \tag{6}$$

here λ denotes the reorganization energy associated with the ET reaction and is given by Eq. (7) [53,54].

$$\lambda = \lambda_i + \lambda_o \tag{7}$$

here λ_i is the inner-sphere reorganization energy due to intramolecular bond length changes and λ_o is the outer-sphere reorganization energy due to reorientation of the solvent molecules. The former may be calculated from the force constants for all the molecular vibrations in both the reactants and products [10]. However, a fixed value of 0.3 eV is often chosen for λ_i. This value of λ_i has been used by several research groups as a characteristic value for aromatic D–A systems [22,55–60]. The value of λ_o is evaluated classically by using dielectric continuum model of two spherical reactants (Eq. (8)) [53,54].

$$\lambda_o = \frac{e^2}{(4\pi\varepsilon_0)}\left[\frac{1}{\varepsilon_{op}} - \frac{1}{\varepsilon_s}\right]\left[\frac{1}{(2r_D)} + \frac{1}{(2r_A)} - \frac{1}{R}\right] \tag{8}$$

here ε_{op} is the solvent refractive index (optical dielectric constant); r_D and r_A are the radii of the oxidized donor and reduced acceptor, respectively. For the present D–A systems, r_D and r_A are 8.8 Å and

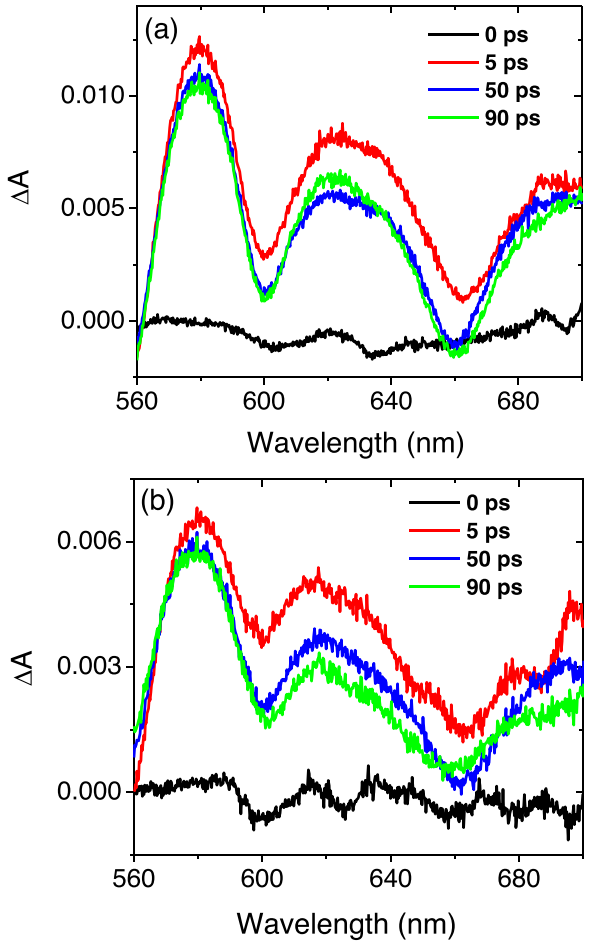

Fig. 7. Transient absorption spectra of ZnTPP (2.0×10^{-5} mol/L) (a) without 2NF and (b) with 2NF (1.2×10^{-2} mol/L) in ACN at different delay times (up to 100 ps) following excitation at 400 nm with a laser pulse.

5.1 Å, respectively, while $R=(r_D+r_A)$ (centre-to-centre distance between donor and acceptor molecules, vide supra). Thus, the calculated value of λ comes out to be equal to 0.924 eV for the D–A system used in the present investigations. This leads to k_{ET} equal to $1.14\times10^{9}\,s^{-1}$ for ZnTPP–2NF system in ACN.

It is well-known [45,52,61,62] that in case of intermolecular ET, the singlet excited donor and ground state acceptor molecules ($D^{*}+A$) first come in close proximity to each other by diffusion, forms an encounter complex ($D^{*}\cdots A$, also called precursor complex) in which ET occurs to give rise to a successor complex ($D^{+}\cdots A^{-}$, also called contact ion pair), which subsequently leads to solvent separated ion pair ($D^{+}+A^{-}$). Applying steady state treatment to the various intermediates associated to the ET reaction, one can compute the fluorescence quenching rate constant, $k_{q(ET)}$, as a consequence of ET reaction from Eq. (9) [45,52,61,62].

$$k_{q(ET)}=\frac{k_d k_{ET}}{k_{-d}+k_{ET}} \tag{9}$$

here k_d and k_{-d} are the diffusion-controlled rate constants of second-order and first-order, respectively. The values of k_d and k_{-d} are calculated by using Debye–Smoluchowski equation and Eigen equation, respectively [63]. In the present case, we obtained $k_d=1.9\times10^{10}\,L/(mol\,s)$ and $k_{-d}=2.7\times10^{9}\,s^{-1}$ in ACN. Therefore, the calculated value of $k_{q(ET)}$ for ZnTPP–2NF system in ACN comes out to be equal to $5.65\times10^{9}\,L/(mol\,s)$, which is slightly less than k_d as predicted by Marcus theory. Moreover, the value of $k_{q(ET)}$ as calculated from Marcus theory agrees excellently with the observed values of k_q obtained from steady state as well as time-resolved (TCSPC) measurements (vide supra). However, it must be mentioned that calculations based on Marcus theory in the present investigations give only a rough estimation of the value of $k_{q(ET)}$ as the values of two parameters (A and λ_i) are taken ad hoc. Moreover, for intermolecular PET, there may be a large dispersion of the value of k_{ET} for different distances between the donor and acceptor molecules in the liquid medium.

3.6. Transient absorption measurements

Fig. 7 shows the transient absorption spectra of ZnTPP in ACN at different delay times (up to 100 ps) following Soret band excitation of ZnTPP without and with 2NF, respectively. Clearly, upon Soret band excitation of ZnTPP, fast (apparently within a few hundred femtoseconds) excited state absorption (ESA) from the S_2 state of ZnTPP to higher electronic states gives rise to a broad transient absorption spectra in 560–700 nm region, which then decay in picosecond time scale due to depopulation of the S_2 state. The moderate reduction of the transient absorption signal at 90 ps delay time compared to that at 5 ps delay time indicates the presence of ESA from the S_1 state of ZnTPP to a large extent. Similar features are observed in the transient absorption spectra of the Soret band excited ZnTPP in presence of 2NF except that the presence of 2NF results in a faster decay of the spectra compared to those in absence of 2NF. In order to verify this, the transient absorption kinetics of the Soret band excited ZnTPP in ACN without and with 2NF are analyzed at a probe wavelength of 620 nm (Fig. 8). Fig. 8 shows that in absence of 2NF, the transient absorption occurs with a rise time constant of $\tau_r=194$ fs, while the decay of the transient absorption follows a triple-exponential fit with two fast (of the order of picoseconds) decay time constants of $\tau_{d1}=2.16$ ps, $\tau_{d2}=25.53$ ps and a third long-lived (of the order of nanoseconds, which could not be resolved in the present time window) component (normalized pre-exponential factors 0.84, 0.07 and 0.09, respectively). The third relatively slower ESA signal was analyzed separately by applying longer time delays up to ca. 7 ns (vide infra). Earlier, Yu et al. [19] reported that the transient

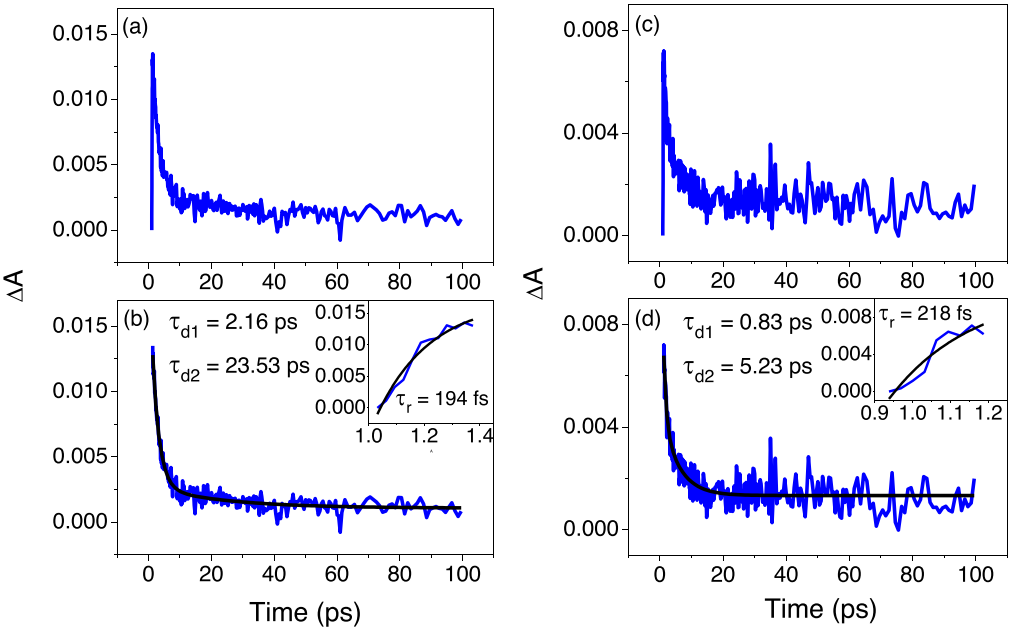

Fig. 8. Transient absorption kinetics of ZnTPP (2.0×10^{-5} mol/L) in ACN following excitation at 400 nm at a probe wavelength of 620 nm (up to a delay time of 100 ps): (a) complete transient absorption kinetics without 2NF; (b) decay of the transient absorption (blue curve) without 2NF and triple-exponential fit (black curve) with two fast time constants of 2.16 ps, 23.53 ps and a third slow one (~ns) (normalized pre-exponential factors 0.82, 0.08 and 0.10, respectively), while the inset shows the rise of the transient absorption (blue curve) and single-exponential fit (black curve) with a time constant of 194 fs; (c) complete transient absorption kinetics with 2NF (1.2×10^{-2} mol/L); (d) decay of the transient absorption (blue curve) with 2NF (1.2×10^{-2} mol/L) and triple-exponential fit (black curve) with two fast time constants of 0.83 ps, 5.23 ps and a third slow one (~ns) (normalized pre-exponential factors 0.66, 0.24 and 0.10, respectively), while the inset shows the rise of the transient absorption (blue curve) and single-exponential fit (black curve) with a time constant of 218 fs. (For interpretation of the references to color in this figure legend, the reader is referred to the web version of this article.)

absorption decay of Soret band excited ZnTPP at a probe wavelength of 656 nm fits well with two picosecond exponential components (1.5 ps and 12 ps in benzene; 2.1 ps and 38 ps in dichloromethane) and a third long-lived (≥nanosecond) contribution. Also, Kumble et al. [64] observed two distinct decay time constants (1.2 ps and 18 ps) along with a third long-lived (>1 ns) one associated with the transient absorption kinetics of ZnTPP, upon photoexcitation at 400 nm, at a probe wavelength of 610 nm in chloroform. Based on their interpretations [19,64], our observed decay time constants of τ_{d1} = 2.16 ps and τ_{d2} = 25.53 ps are ascribed to be due to the relaxation of the S_2 state to the S_1 state by internal conversion (IC), followed by a slower vibrational relaxation (vibrational cooling, VC) in the S_1 state by energy loss to the solvent ACN. The third long-lived (of the order of nanoseconds) decay component is attributed to the ESA from the S_1 state (zero vibrational level) to higher electronic states (including S_2 state) of ZnTPP. Interestingly, in presence of 2NF, the transient absorption occurs with τ_r = 218 fs, while the decay of the transient absorption follows a triple-exponential fit with the two fast components τ_{d1} = 0.83 ps, τ_{d2} = 5.23 ps and a third slow component (normalized pre-exponential factors 0.69, 0.20 and 0.11, respectively) (Fig. 8). Thus, the ultrafast formation kinetics of the ESA signal from the S_2 state of ZnTPP to higher electronic states are not affected by the presence of 2NF. However, the decay time constants (τ_{d1} and τ_{d2}) become 3–5 times faster in presence of 2NF than in absence of 2NF.

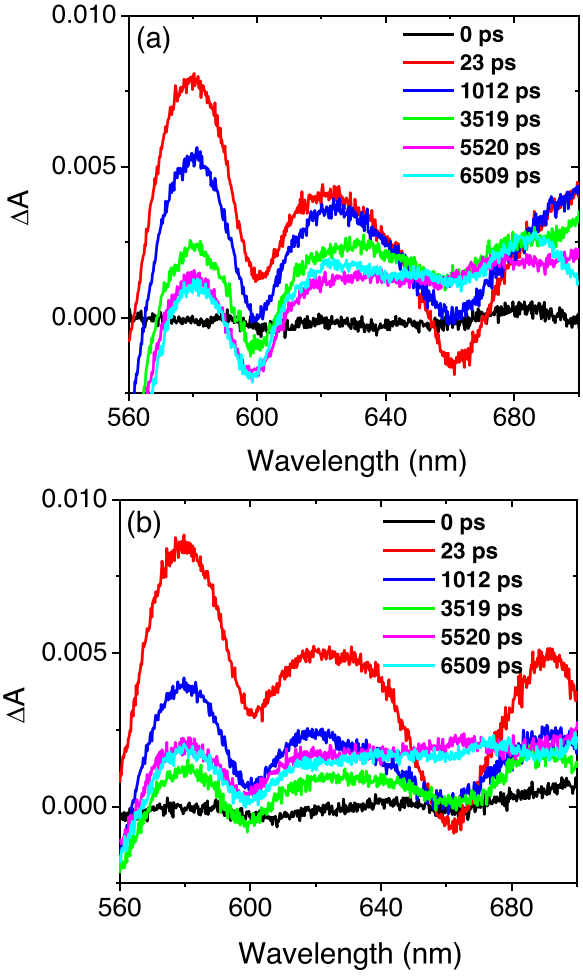

Fig. 9. Transient absorption spectra of ZnTPP (2.0×10^{-5} mol/L) (a) without 2NF and (b) with 2NF (1.2×10^{-2} mol/L) in ACN at different delay times (up to ca. 7 ns) following excitation at 400 nm with a laser pulse.

Obviously, this indicates ultrafast ET from the S_2 state (zero vibrational level) as well as the higher vibrational levels of the S_1 state of ZnTPP to 2NF in ACN. Treating the two ET processes independently, as a first approximation, the ET rate constants calculated from the observed values of τ_{d1} and τ_{d2} without and with 2NF are found to be equal to 7.4×10^{11} s^{-1} and 1.5×10^{11} s^{-1}, respectively. These ET processes should give rise to ultrafast formation and subsequent decay of ZnTPP radical cation, which is known to have a broad transient absorption spectra in 600–700 nm region (approximately) [11,14–17,21]. However, no such distinct band could be detected probably due to: (i) the transient absorption spectra of ZnTPP radical cation overlap with the spectra of the ESA from the S_2 state as well as the higher vibrational levels of the S_1 state of ZnTPP; (ii) the transient absorption of ZnTPP radical cation decays in picosecond time scale, thereby making it difficult to distinguish this decay kinetics with that of the ESA from the S_2 state as well as the higher vibrational levels of the S_1 state of ZnTPP. Robotham et al. [25] reported similar rapid formation and fast decay (within a few picoseconds) of ZnTPP radical cation due to ET from the S_2 state of the Soret band excited ZnTPP to the covalently linked ANDI acceptor in BN and toluene solvents. Therefore, the observed values of τ_{d1} and τ_{d2} in presence of 2NF may not represent the proper decays of the ESA signal from the S_2 state as well as the higher vibrational levels of the S_1 state of ZnTPP. Hence, the presently calculated ET rates may not give true pictures regarding the ET processes from the S_2 state as well as the higher vibrational levels of the S_1 state of ZnTPP to 2NF and, at best, may be treated as approximate values.

Fig. 9 shows the transient absorption spectra of ZnTPP in ACN at longer delay times (first at 23 ps and then increasing at regular intervals up to ca. 7 ns) following Soret band excitation of ZnTPP without and with 2NF, respectively. As ESA from the S_2 state of ZnTPP to higher electronic states decays in a few picoseconds and the first time delay is at 23 ps, Fig. 9 shows ESA from the S_1 state of

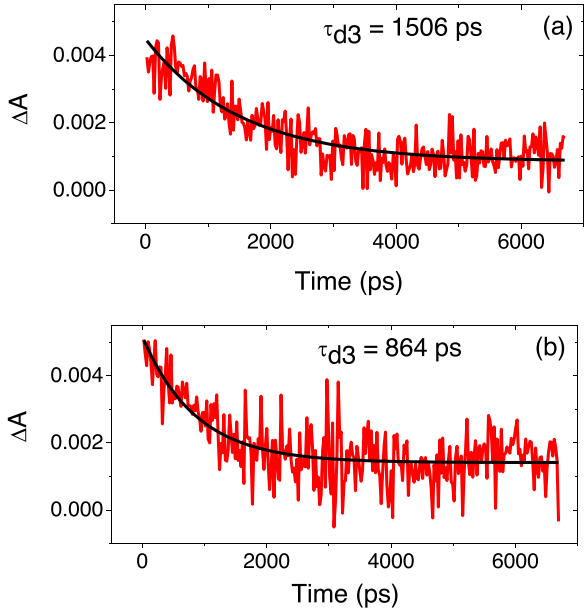

Fig. 10. Transient absorption kinetics of ZnTPP (2.0×10^{-5} mol/L) in ACN following excitation at 400 nm (up to a delay of ca. 7 ns) at a probe wavelength of 620 nm: (a) without 2NF; (b) with 2NF (1.2×10^{-2} mol/L). Red curve represents the original transient absorption decay and black curve represents the single-exponential fit with decay time constants of (a) 1506 ps; (b) 864 ps. (For interpretation of the references to color in this figure legend, the reader is referred to the web version of this article.)

Soret band excited ZnTPP to higher electronic states giving rise to a broad transient absorption spectra in 560–700 nm region. The ESA signal decays almost completely by ca. 5.5 ns and then remains nearly the same in intensity up to ca. 6.5 ns. On the other hand, in presence of 2NF, the ESA signal (from the S_1 state to the higher electronic states) of ZnTPP decays faster so as to decay appreciably by ca. 3.5 ns (Fig. 9). Then, beyond ca. 3.5 ns, a rising broad transient absorption spectra is observed at about 5.5 ns in 560–700 nm region, which decays slowly at further time delays up to ca. 6.5 ns. This rising and subsequent decaying broad transient absorption spectra is attributed to the formation and subsequent decay of ZnTPP radical cation [11,14–17,21] due to ET from the S_1 state (zero vibrational level) of ZnTPP to 2NF. In order to verify this conjecture, we analyzed the transient absorption kinetics of the Soret band excited ZnTPP at a probe wavelength of 620 nm without and with 2NF. In absence of 2NF, the transient absorption signal at 620 nm follows single-exponential fit with decay time constant (τ_{d3}) of 1506 ps (Fig. 10a). The S_1 state of ZnTPP may depopulate via radiative deactivation (fluorescence) to the ground state (S_0) and non-radiative deactivation (intersystem crossing, ISC) to the first excited triplet state (T_1). The fluorescence lifetime of the S_1 state of ZnTPP is 1.91 ns (Table 1). Again, ISC from the S_1 state of ZnTPP to the T_1 state occurs with a rate constant ~2 ns [19,65]. Therefore, the decay of the ESA from the S_1 state of ZnTPP to higher electronic states due to depopulation of the S_1 state is expected to yield a time constant ~1–2 ns. This is in perfect agreement with the observed value of τ_{d3} at 620 nm. Fig. 10b shows that the transient absorption kinetics at 620 nm in presence of 2NF give a value of τ_{d3} equal to 864 ps, when fitted with a single-exponential decay function. However, the fit is moderately good only up to ca. 4 ns and becomes really bad beyond 4 ns. Also, Fig. 10b clearly indicates that there is a decay component up to ca. 4 ns and then a rising component up to ca. 5.5 ns followed by a decay component up to ca. 6.7 ns. Accordingly, the transient absorption kinetics at 620 nm in presence of 2NF are re-analyzed as shown in Fig. 11. At a probe wavelength of 620 nm, we observe an initial decay component (Fig. 11b), then a rising component (Fig. 11c) followed by a decay component (Fig. 11d). It is to be noted that the signal related to the intrinsic deactivation of the S_1 state of ZnTPP overlaps with the rising followed by decaying signal of ZnTPP radical cation. The presence of the latter part (weak rising followed by weak decaying signal of ZnTPP radical cation) seems to be masked up to ca. 4 ns by the relatively intense decaying ESA signal and becomes distinctly observable beyond ca. 4 ns. In fact, even beyond ca. 4 ns, the decaying ESA signal may appreciably affect the rising as well as decaying signal of ZnTPP radical cation. Thus, the rising and decaying signals of ZnTPP radical cation shown in Fig. 11c and d, respectively, may, at best, be treated as approximate qualitative ones. Hence, we refrain in fitting the rising and decaying signals of ZnTPP radical cation with single-exponential functions. However, presence of the weak rising and weak decaying signals of ZnTPP radical cation is expected not to affect the decaying ESA signal significantly in the initial part (up to ca. 4 ns) of the transient absorption kinetics. Therefore, single-exponential fitting of the initial decay component giving rise to τ_{d3} = 1015 ps (Fig. 11b) may be treated as an approximate quantitative one. Obviously, τ_{d3} = 1015 ps is due to the accelerated decay of the ESA signal at 620 nm from the S_1 state to the higher electronic states of ZnTPP in presence of 2NF, indicating slow ET from the S_1 state (zero vibrational level) of ZnTPP to 2NF with a rate constant $3.2 \times 10^8\ s^{-1}$ (approximately). Consequently, a CS state is formed leading to the rise of the transient absorption signal of ZnTPP radical cation followed by a decaying signal due to geminate recombination. Thus, our transient absorption measurements at longer time delays clearly show the formation of a CS state due to ET from the S_1 state of the Soret excited ZnTPP to 2NF in ACN.

Fig. 12 shows a comprehensive kinetic scheme indicating the aforementioned various possible photophysical pathways in the transient absorption measurements of (ZnTPP + 2NF) system. Here, τ_r is the ultrafast (of the order of few hundred femtoseconds) rise of the ESA signal from the S_2 state (zero vibrational level) to higher singlet states of ZnTPP upon Soret band excitation at 400 nm. IC from the zero vibrational level of the S_2 state to the higher vibrational levels of the S_1 state of ZnTPP and VC from the higher vibrational levels to the zero vibrational level of the S_1 state of ZnTPP are responsible for τ_{d1} and τ_{d2}, respectively. Radiative (fluorescence) and non-radiative (ISC) deactivations of the S_1 state (zero vibrational level) of ZnTPP are collectively responsible for τ_{d3}.

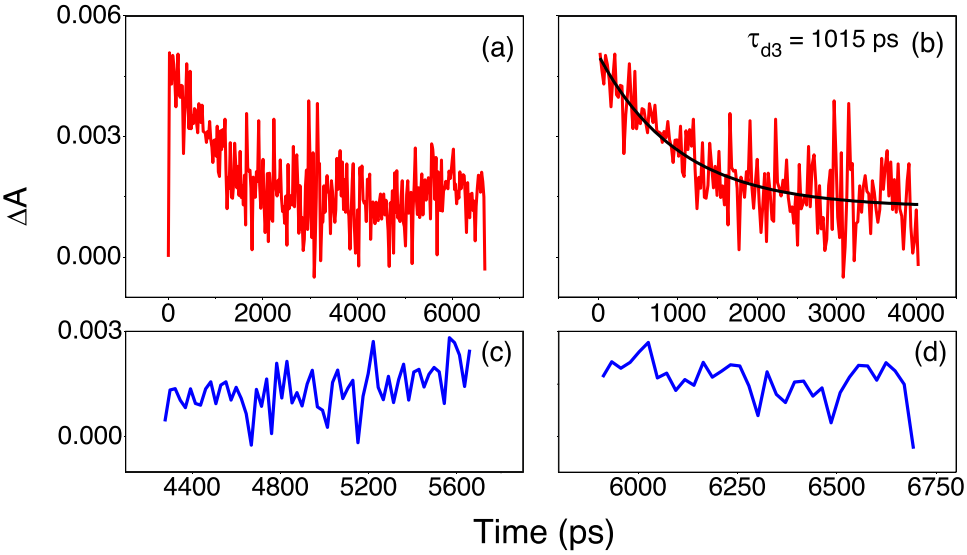

Fig. 11. Transient absorption kinetics of ZnTPP (2.0×10^{-5} mol/L) in presence of 2NF (1.2×10^{-2} mol/L) in ACN following excitation at 400 nm at a probe wavelength of 620 nm: (a) complete transient absorption kinetics up to a delay of ca. 7 ns; (b) decay of the transient absorption (red curve) in the range 23–4025 ps and single-exponential fit (black curve) with a time constant of 1015 ps; (c) rise of the transient absorption (blue curve) in the range 4278–5658 ps; (d) decay of the transient absorption (blue curve) in the range 5911–6693 ps. (For interpretation of the references to color in this figure legend, the reader is referred to the web version of this article.)

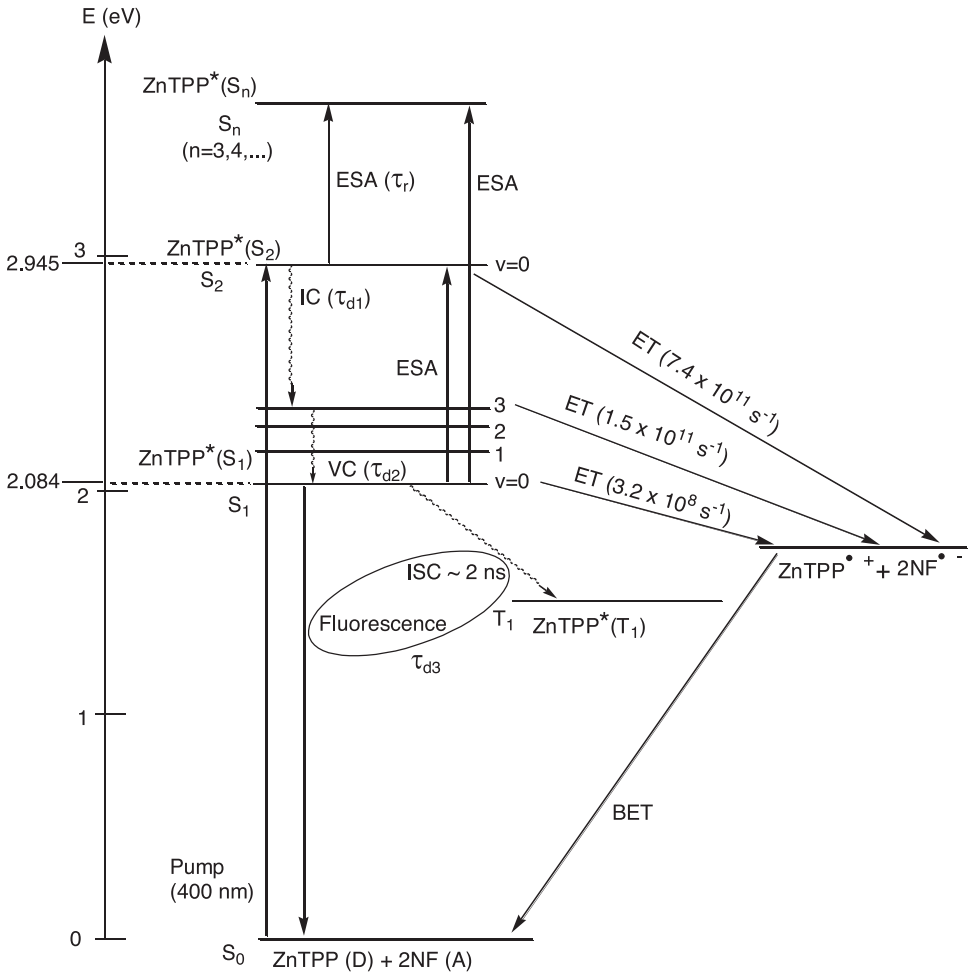

Fig. 12. Kinetic scheme showing the various possible photophysical pathways in the transient absorption measurements of (ZnTPP + 2NF) system (see text). Here, BET stands for back electron transfer.

All the three decay rates (τ_{d1},τ_{d2} and τ_{d3}) are accelerated in presence of 2NF. Thus, our transient absorption data suggest three possible pathways of PET from Soret-excited ZnTPP to 2NF: (a) from the zero vibrational level of the S_1 state of ZnTPP to 2NF with a rate $3.2 \times 10^8\ s^{-1}$, (b) from the higher vibrational levels of the S_1 state of ZnTPP to 2NF with a rate $1.5 \times 10^{11}\ s^{-1}$ (ultrafast) and (c) from the zero vibrational level of the S_2 state of ZnTPP to 2NF with a rate $7.4 \times 10^{11}\ s^{-1}$ (ultrafast).

Finally, it is to be mentioned that we carried out kinetic analysis of the transient absorption data for ZnTPP and (ZnTPP + 2NF) systems at a probe wavelength of 620 nm in spite of the fact that several pathways like ESA from the S_1 and S_2 states of ZnTPP, stimulated emission (SE) from the S_1 state of ZnTPP and absorption due to ZnTPP radical cation contribute to the transient absorption signal at the probe wavelength of 620 nm to different extents. Till date, many research groups analyzed the kinetics of the transient absorption data for various ZnTPP based D–A systems with different acceptors at some specific probe wavelengths [12,14–19,21,64]. Here, we made an attempt to quantitatively (though not too precise) analyze the kinetics of the transient absorption data at a single probe wavelength of 620 nm based on the following facts: (i) one of the peak positions of the ESA signal from the S_1 and S_2 states of ZnTPP is at 620 nm; (ii) the chosen probe wavelength of 620 nm is almost at the middle of the broad transient absorption spectra due to ESA from the S_1 and S_2 states of ZnTPP; (iii) the SE signal from the S_1 state of ZnTPP mostly contributes at about 600 nm and 650 nm and its contribution at 620 nm is nearly the least.

4. Conclusions

In the present work, we report the possibility of the occurrence of intermolecular PET in a novel porphyrin based D–A system (ZnTPP–2NF) in polar solvent ACN. Our steady state as well as time-resolved (TCSPC and femtosecond transient absorption) data show that intermolecular PET indeed occurs from the S_1 and S_2 states of singlet excited ZnTPP to 2NF. The transient absorption kinetics are analyzed very carefully to show the formation of a CS state (though albeit indirectly). It is to be noted that the presently used acceptor 2NF may be easily obtained in the market at relatively very low cost compared to some traditionally used acceptors like C_{60}. Thus, the D–A system used in the present investigations for studying PET seems to be quite promising candidate for the realization of novel organic photovoltaics, which can be commercialized easily on a wide scale due to the low price involved in the manufacturing process.

Acknowledgment

Subrata Sinha acknowledges the Department of Atomic Energy (DAE) – Board of Research in Nuclear Sciences (BRNS), India

(Project No.: 2010/37P/12/BRNS) for providing financial assistances in the form of grants and fellowship.

References

[1] M. Gouterman, The Porphyrins, vol. III, Academic Press, New York, 1978.
[2] Anoxygenic Photosynthetic Bacteria, in: R.E. Blankenship, M.T. Madigan, C.E. Bauer (Eds.), Kluwer Academic Publishers, Dordrecht, 1995.
[3] G.T. Babcock, How oxygen is activated and reduced in respiration, Proc. Natl. Acad. Sci. U. S. A. 96 (1999) 12971–12973.
[4] K.M. Kadish, K.M. Smith, R. Guiard (Eds.), The Porphyrin Handbook, vols. 1–20, Academic Press, New York, 2003.
[5] S. Fukuzumi, K. Okamoto, C.P. Gros, R. Guilard, Mechanism of four-electron reduction of dioxygen to water by ferrocene derivatives in the presence of perchloric acid in benzonitrile, catalyzed by cofacial dicobalt porphyrins, J. Am. Chem. Soc. 126 (2004) 10441–10449.
[6] S. Hammes-Schiffer, Theory of proton-coupled electron transfer in energy conversion processes, Acc. Chem. Res. 42 (2009) 1881–1889.
[7] H.B. Gray, J.R. Winkler, Electron flow through metalloproteins, Biochim. Biophys. Acta Bioenerg. 1797 (2010) 1563–1572.
[8] J. Deisenhofer, J.R. Norris (Eds.), The Photosynthetic Reaction Center, vols. I and II, Academic Press, New York, 1993.
[9] P. Heathcote, P.K. Fyfe, M.R. Jones, Reaction centres: the structure and evolution of biological solar power, Trends Biochem. Sci. 27 (2002) 79–87.
[10] M.R. Wasielewski, Photoinduced electron transfer in supramolecular systems for artificial photosynthesis, Chem. Rev. 92 (1992) 435–461.
[11] D. Kuciauskas, S. Lin, G.R. Seely, A.L. Moore, T.A. Moore, D. Gust, T. Drovetskaya, C.A. Reed, P.D.W. Boyd, Energy and photoinduced electron transfer in porphyrin–fullerene dyads, J. Phys. Chem. 100 (1996) 15926–15932.
[12] T.D.M. Bell, T.A. Smith, K.P. Ghiggino, M.G. Ranasinghe, M.J. Shephard, M.N. Paddon-Row, Long-lived photoinduced charge separation in a bridged C_{60}-porphyrin dyad, Chem. Phys. Lett. 268 (1997) 223–228.
[13] J.L. Bahr, D. Kuciauskas, P.A. Liddell, A.L. Moore, T.A. Moore, D. Gust, Driving force and electronic coupling effects on photoinduced electron transfer in a fullerene-based molecular triad, Photochem. Photobiol. 72 (2000) 598–611.
[14] C. Luo, D.M. Guldi, H. Imahori, K. Tamaki, Y. Sakata, Sequential energy and electron transfer in an artificial reaction center: formation of a long-lived charge-separated state, J. Am. Chem. Soc. 122 (2000) 6535–6551.
[15] H. Imahori, K. Tamaki, D.M. Guldi, C. Luo, M. Fujitsuka, O. Ito, Y. Sakata, S. Fukuzumi, Modulating charge separation and charge recombination dynamics in porphyrin–fullerene linked dyads and triads: Marcus-normal versus inverted region, J. Am. Chem. Soc. 123 (2001) 2607–2617.
[16] H. Imahori, M.E. El-Khouly, M. Fujitsuka, O. Ito, Y. Sakata, S. Fukuzumi, Solvent dependence of charge separation and charge recombination rates in porphyrin–fullerene dyad, J. Phys. Chem. A 105 (2001) 325–332.
[17] T.D.M. Bell, K.P. Ghiggino, K.A. Jolliffe, M.G. Ranasinghe, S.J. Langford, M.J. Shephard, M.N. Paddon-Row, Photoinduced energy and electron transfer in a giant zinc porphyrin-bridge-C_{60} system, J. Phys. Chem. A 106 (2002) 10079–10088.
[18] T. Van der Boom, R.T. Hayes, Y. Zhao, P.J. Bushard, E.A. Weiss, M.R. Wasielewski, Charge transport in photofunctional nanoparticles self-assembled from zinc 5,10,15,20-tetrakis(perylenediimide) porphyrin building blocks, J. Am. Chem. Soc. 124 (2002) 9582–9590.
[19] H.-Z. Yu, S. Baskin, A.H. Zewail, Ultrafast dynamics of porphyrins in the condensed phase: II. Zinc tetraphenylporphyrin, J. Phys. Chem. A 106 (2002) 9845–9854.
[20] R.P. Steer, Concerning correct and incorrect assignments of Soret (S2–S0) fluorescence in porphyrinoids: a short critical review, Photochem. Photobiol. Sci. 13 (2014) 1117–1122.
[21] R.T. Hayes, C.J. Walsh, M.R. Wasielewski, Competitive electron transfer from the S2 and S1 excited states of zinc meso-tetraphenylporphyrin to a covalently bound pyromellitimide: dependence on donor-acceptor structure and solvent, J. Phys. Chem. A 108 (2004) 2375–2381.
[22] P. Mandal, S.K. Tiwari, T. Ganguly, S. Sinha, Fluorescence quenching of 9-cyanoanthracene in presence of zinc tetraphenylporphyrin in a polar liquid medium, J. Lumin. 129 (2009) 958–965.
[23] H.M. Zeyada, M.M. El-Nahass, M.A. Ali, Transport mechanisms and photovoltaic properties of zinc tetraphenylporphyrin/n-type silicon heterojunction solar cell, Eur. Phys. J. Appl. Phys. 56 (2011) 10201–10208.
[24] M. Kanematsu, P. Naumov, T. Kojima, S. Fukuzumi, Intermolecular and intracomplex photoinduced electron transfer from planar and nonplanar metalloporphyrins to *p*-quinones, Chem. Eur. J. 17 (2011) 12372–12384.
[25] B. Robotham, K.A. Lastman, S.J. Langford, K.P. Ghiggino, Ultrafast electron transfer in a porphyrin-amino naphthalene diimide dyad, J. Photochem. Photobiol. A: Chem. 251 (2013) 167–174.
[26] D. Villamaina, S.V. Bhosale, S.J. Langford, E. Vauthry, Excited-state dynamics of porphyrin–naphthalenediimide–porphyrin triads, Phys. Chem. Chem. Phys. 15 (2013) 1177–1187.
[27] J. Wienke, T.J. Schaafsma, Visible light sensitization of titanium dioxide with self-organized porphyrins: organic P-I-N solar cells, J. Phys. Chem. B 103 (1999) 2702–2708.
[28] S. Rai, M. Ravikan, Synthesis and fluorescence properties of covalently linked homo- and hetero-porphyrin dyads containing meso-tolyl porphyrin and meso-furyl porphyrin sub-units, Tetrahedron 63 (2007) 2455–2465.
[29] L. Flamigni, B. Ventura, M. Tasior, D.T. Gryko, Photophysical properties of a new, stable corrole-porphyrin dyad, Inorg. Chim. Acta 360 (2007) 803–813.
[30] M.O. Senge, M. Pazekas, E.G.A. Notaras, W.J. Blau, M. Zawadzka, O.B. Locos, E.M. N. Mhuircheartaigh, Nonlinear optical properties of porphyrins, Adv. Mater. 19 (2007) 2737–2774.
[31] R. Matsumoto, T. Nagamura, N. Aratani, T. Ikeda, A. Osuka, Ultrafast all-optical light modulation in the near infrared region by phase sensitive polymer guided wave mode geometry containing porphyrin tapes, Appl. Phys. Lett. 94 (2009) 253301-1–253301-3.
[32] C.D. Natale, R. Paolesse, M. Burgio, E. Martinelli, G. Pennazza, A. Amico, Application of metalloporphyrins-based gas and liquid sensor arrays to the analysis of red wine, Anal. Chem. Acta 513 (2004) 49–56.
[33] O.V. Khodykin, S.J. Zilker, D. Haarer, B.M. Kharlamov, Zinc-tetrabenzoporphyrine-doped poly(methyl methacrylate): a new photochromic recording medium, Opt. Lett. 24 (1999) 513–515.
[34] Metalloporphyrins in Catalytic Oxidations, in: F. Montanari, L. Casella (Eds.), Kluwer Academic, Dordrecht, 1994.
[35] T. Aida, S. Inoue, Metalloporphyrins as initiators for living and immortal polymerizations, Acc. Chem. Res. 29 (1996) 39–48.
[36] M.G.H. Vicente, Porphyrin-based sensitizers in the detection and treatment of cancer: recent progress, Curr. Med. Chem.-Anti-Cancer Agents 1 (2001) 175–194.
[37] S. Rywkin, E. Ben-Hur, Z. Malik, A.M. Prince, Y.-S. Li, M.E. Kenney, N.L. Oleinik, B. Horowitz, New phthalocyanines for photodynamic virus inactivation in red blood cell concentrates, Photochem. Photobiol. 60 (1994) 165–170.
[38] E. Ben-Hur, B. Horowitz, Advances in photochemical approaches for blood sterilization, Photochem. Photobiol. 62 (1995) 383–388.
[39] H. Brunner, K.M. Schellerer, Benzoporphyrins and acetylene-substituted porphyrins as improved photosensitizers in the photodynamic tumor therapy with porphyrin platinum conjugates, Monatsh. Chem. 133 (2002) 679–705.
[40] W. Li, W. Lu, Z. Fan, X. Zhu, A. Reed, B. Newton, Y. Zhang, S. Courtney, P.T. Tiyyagura, S. Li, E. Butler, H. Yu, P.C. Ray, R. Gao, Enhanced photodynamic selectivity of nano-silica-attached porphyrins against breast cancer cells, J. Mater. Chem. 22 (2012) 12701–12708.
[41] R.A. Binstead, M.J. Crossley, N.S. Hush, Modulation of valence orbital levels of metalloporphyrins by beta-substitution: evidence from spectroscopic and electrochemical studies of 2-substituted metallo-5,10,15,20-tetraphenylporphyrins, Inorg. Chem. 30 (1991) 1259–1264.
[42] D.J. Quimby, F.R. Longo, Luminescence studies on several tetraarylporphins and their zinc derivatives, J. Am. Chem. Soc. 97 (1975) 5111–5117.
[43] M. Ghosh, S. Nath, A. Hajra, S. Sinha, Fluorescence self-quenching of tetraphenylporphyrin in liquid medium, J. Lumin. 141 (2013) 87–92.
[44] M. Ghosh, A.K. Mora, S. Nath, A.K. Chandra, A. Hajra, S. Sinha, Photophysics of Soret-excited free base tetraphenylporphyrin and its zinc analog in solution, Spectrochim. Acta A: Mol. Biomol. Spectrosc. 116 (2013) 466–472.
[45] S. Sinha, R. De, T. Ganguly, Electron transfer reactions in the excited singlet states of dimethyl substituted phenol-2-nitrofluorene systems: evidence for the Marcus inverted region and concurrent occurrence of energy transfer processes, J. Phys. Chem. A 101 (1997) 2852–2858.
[46] S. Sinha, R. De, T. Ganguly, A.K. De, S.K. Nandy, Studies on quenching reactions on the excited electronic states of tetrahydronaphthols both at the ambient temperature as well as at 77 K, J. Lumin. 75 (1997) 99–116.
[47] S. Sinha, T. Ganguly, Investigations on the nature of non-radiative transitions from excited singlet and triplet states of dimethyl substituted phenols in the presence of acceptor 2-nitrofluorene at 77 K, J. Photochem. Photobiol. A: Chem. 117 (1998) 83–90.
[48] S. Sinha, T. Ganguly, Investigations on the photophysical properties of 2-methylindole and 2-methylindoline in various environments. Studies on the nature of non-radiative transitions in presence of the electron acceptor 2-nitrofluorene, J. Lumin. 79 (1998) 201–209.
[49] D. Rehm, A. Weller, Kinetics of fluorescence quenching by electron and H-atom transfer, Isr. J. Chem. 8 (1970) 259–271.
[50] J.-H. Fuhrhop, K.M. Kadish, D.G. Davis, Redox behavior of metallo oxtaethylporhyrins, J. Am. Chem. Soc. 95 (1973) 5140–5147.
[51] J.R. Lakowicz, Principles of Fluorescence Spectroscopy, 2nd ed., Kluwer Academic/Plenum Publishers, New York, 1999.
[52] J. Chen, T. Ho, C. Mou, Experimental investigation of excited-state electron-transfer reaction: effects of free energy and solvent on rates, J. Phys. Chem. 94 (1990) 2889–2896.
[53] R.A. Marcus, On the theory of oxidation–reduction reactions involving electron transfer, J. Chem. Phys. 24 (1956) 966–978.
[54] R.A. Marcus, N. Sutin, Spin and electron distributions in heme-cyanide models and hemeproteins, Biochim. Biophys. Acta 811 (1985) 265–273.
[55] J.R. Miller, L.T. Calcaterra, G.C. Closs, Intramolecular long-distance electron transfer in radical anions. The effects of free energy and solvent on the reaction rates, J. Am. Chem. Soc. 106 (1984) 3047–3049.
[56] G.L. Closs, M.D. Johnson, J.R. Miller, P. Piotrowiack, A connection between intramolecular long-range electron, hole and triplet energy transfers, J. Am. Chem. Soc. 111 (1989) 3751–3753.
[57] I.R. Gould, D. Ege, J.E. Moser, S. Farid, Efficiencies of photoinduced electron-transfer reactions: role of the Marcus inverted region in return electron transfer within geminate radical-ion pairs, J. Am. Chem. Soc. 112 (1990) 4290–4301.
[58] J.M. Warman, K.J. Smit, M.P. De Haas, S.A. Jonker, M.N. Paddon-Row, A.N. Oliver, J. Kroon, H. Oevering, J.W. Verhoeven, Long-distance charge recombination within rigid molecular assemblies in nondipolar solvents, J. Phys. Chem. 95 (1991) 1979–1987.

[59] I.R. Gould, R.H. Young, R.G. Moody, S. Farid, Contact and solvent-separated geminate radical ion pairs in electron-transfer photochemistry, J. Phys. Chem. 95 (1991) 2068–2080.
[60] T. Ganguly, D.K. Sharma, S. Gauthier, D. Gravel, G. Durocher, Strongly exothermic electron-transfer reaction in the excited singlet state of alkylcarbazole-polynitrofluorene and -polynitrofluorenone bichromophoric systems. 1. Correlation between the probability of charge separation, photoactivity and picosecond laser photolysis studies on the photoinduced charge recombination of ion pair state produced in some media, J. Phys. Chem. 96 (1992) 3757–3766.
[61] N. Sutin, Nuclear, electronic and frequency factors in electron transfer reactions, Acc. Chem. Res. 15 (1982) 275–282.
[62] S.A. Rice, Diffusion Limited Reaction, Comprehensive Chemical Kinetics, in: C.A. Bamford, C.F.H. Tipper, R.G. Compton (Eds.), Elsevier, Amsterdam, 1985.
[63] B. Marciniak, K. Bobrowski, G.L. Hug, Quenching of triplet states of aromatic ketones by sulfur-containing amino acids in solution. Evidence for electron transfer, J. Phys. Chem. 97 (1993) 11937–11943.
[64] R. Kumble, S. Palese, S.Y.V. Lin, M.J. Therien, R.M. Hochstrasser, Ultrafast dynamics of highly conjugated porphyrin arrays, J. Am. Chem. Soc. 120 (1998) 11489–11498.
[65] S.A. Vail, P.J. Krawczuk, D.M. Guldi, A. Palkar, L. Echegoyen, J.P.C. Tomé, M.A. Fazio, D.I. Schuster, Energy and electron transfer in polyacetylene-linked zinc–porphyrin–[60] fullerene molecular wires, Chem. Eur. J. 11 (2005) 3375–3388.